ARTICLE

ACS chemical biology

Mutagenesis of a Modular Polyketide Synthase Enoylreductase Domain Reveals Insights into Catalysis and Stereospecificity

David H. Kwan*,† and Peter F. Leadlay

Department of Biochemistry, University of Cambridge, 80 Tennis Court Road, Cambridge, United Kingdom CB2 1GA. †Current address: Department of Chemistry, University of British Columbia, 2036 Main Mall, Vancouver, BC, Canada V6T 1Z1

ABSTRACT Modular type I polyketide synthases (PKSs) such as the 6-deoxyerythronolide B synthase (DEBS) or the rapamycin synthase (RAPS) biosynthesize their polyketide products in a fashion similar to fatty acid biosynthesis. Each module of these enzymes consists of multiple catalytic domains. The constituent enoylreductase (ER) domain of a given module stereospecifically reduces an enzyme-bound 2-enoyl intermediate. In a recombinant model PKS containing an ER domain derived from module 13 of RAPS, we have previously used site-specific mutagenesis to identify a key active site residue that influences the stereochemistry of enoylreduction. In this study we have identified further residues involved in stereospecificity. We show here that several other residues, previously considered as catalytically important in the medium-chain dehydrogenase/reductase family of enzymes to which PKS ERs belong, are not essential for enoylreduction in polyketide biosynthesis. However, our results suggest that a lysine residue, also modeled to lie at the active site, might serve as a proton donor to the C-2 position during enoylreduction, as previously proposed for an analogously placed lysine in mammalian fatty acid synthase. These findings further highlight the close mechanistic link between fatty acid and polyketide synthases and provide useful guidance for future biosynthetic engineering of complex polyketide biosynthesis.

Polyketides are a large and important class of natural products biosynthesized by fungi, plants, and bacteria, starting from short-chain carboxylic acids. Between them, these polyketide products exhibit a diverse spectrum of biological activities, including antibiotic, antifungal, antineoplastic, immunosuppressive, and cholesterol-lowering properties (*1*). The biosynthesis of complex polyketides, typified by the antibiotic erythromycin A and the immunosuppressant rapamycin, is catalyzed in bacteria by giant multifunctional enzymes known as modular type I polyketide synthases (PKSs) in a fashion that is highly reminiscent of fatty acid biosynthesis on the mammalian fatty acid synthase (FAS) (*2, 3*). In both cases, the metabolites are assembled through the successive head-to-tail condensation of acyl-CoA esters, without intermediates being released from the multienzyme. However, PKSs utilize a larger pool of precursors for biosynthesis than their FAS counterparts, unusual starter units can be incorporated into the polyketide chain (*4, 5*), and different extender units may also be used to extend the nascent polyketide chain (*6*). Furthermore, in contrast to fatty acid biosynthesis, in which an initially formed β-ketoacyl intermediate is always fully reduced to a fatty acyl group by the successive operation of ketoreductase (KR), dehydratase (DH), and enoylreductase (ER) domains, the degree of reduction of the β-ketoacyl intermediate in polyketide biosynthesis may vary, generating a ketone, hydroxyl, olefin, or saturated methylene at specific positions (*1, 3*). This control is achieved by the organization of modular PKSs into multiple modules, each of which normally catalyzes a single particular cycle of chain extension. Each module contains

*Corresponding author, dkwan@chem.ubc.ca.

Received for review June 16, 2010 and accepted July 13, 2010.

Published online July 13, 2010

10.1021/cb100175a

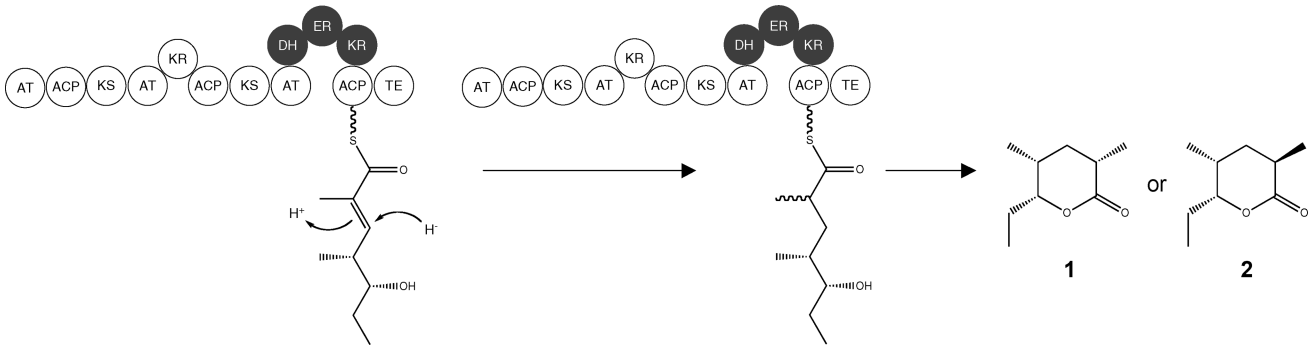

Figure 1. ER-catalyzed reduction of an enzyme-bound 2-enoyl thioester substrate in a triketide synthase and subsequent cyclization. The ER catalyzes the reduction of the carbon–carbon double bond by delivering a hydride to C-3 and a proton to C-2. The resulting triketide 1 or 2 has a methylene at the C-3 position and a methyl substituent at the C-2 position with either *S* or *R* configuration.

ketoacyl-ACP synthase (KS), acyltransferase (AT), and acyl carrier protein (ACP) domains, and some, all, or none of the "reductive domains" (KR, DH, and ER). The modules are organized in the multienzyme in the order they are used, and this assembly line arrangement directly determines the oxidation level at different β-carbon-derived centers within the polyketide. Modular PKSs also generate an impressive diversity of asymmetric centers in their polyketide products. In recent years considerable progress has been made in understanding how the stereochemistry of polyketide chain extension is controlled (*7*) and in relating these outcomes to the intrinsic stereospecificity of individual domains. In the case of KR domains, for example, amino acid sequence motifs have been identified that correlate well with the observed stereochemical outcome (*8, 9*). The significance of these motifs has been confirmed by functional analysis (*10–12*) and determination of the X-ray crystal structure (*13, 14*) of isolated KR domains.

In comparison, the role of enoylreductase (ER) domains in determining the stereochemistry of α-methyl branching in fully reduced ketide units has been little studied. The ER domains of modular PKSs, like the ER domains of mammalian FAS, belong to the NAD(P)H-dependent medium-chain dehydrogenase/reductase (MDR) superfamily of enzymes (*15–17*). The ER domain catalyzes the reduction of the carbon−carbon double bond of a 2-enoyl enzyme bound thioester substrate by delivering a hydride from NADPH to the C-3 position and subsequently delivering a proton to the resulting carbanion intermediate at the C-2 position of the substrate (*18*). Recently, we reported that a single amino acid residue appears to play a key role in determining the stereospecificity *in vivo* of the ER domain (*19*) and showed that site-specific alteration of this residue may switch the configuration of the polyketide produced by the PKS. For modular PKS ER domains in which the residue at position 52′ (corresponding to Tyr52 of the homologous MDR enzyme *E. coli* quinone reductase) is tyrosine, the stereochemical outcome is consistently found to favor the formation of a (2*S*)-alkyl-branched product, whereas in ERs in which the tyrosine at position 52′ is absent and replaced either by valine, alanine, or phenylalanine, the formation of a (2*R*) product is almost invariably observed (*19*). Unfortunately, an isolated PKS ER domain has not yet been obtained in active form, and there is as yet no X-ray crystal structure available, so the role of other active site residues in catalysis remains unclear. However, the recently published X-ray crystal structure of mammalian FAS has revealed the architecture of the ER domain in that multienzyme at 3.2 Å resolution (*17*) and has helped further to validate our homology model (*19*) for the ER of the erythromycin PKS. Here, we report the use of site-specific mutagenesis to probe, *in vivo*, those conserved active site residues in the PKS ER that may influence stereochemistry or that appear from our model to be well-placed to play a catalytic role. We have also examined other residues that have been previously suggested to perform a key role in reduction, in the medium-chain dehydrogenase/reductase (MDR) superfamily of enzymes to which the ER domains of modular PKSs belong (*15–17*), in an effort to gain an insight into common features of catalysis in this family of enzymes.

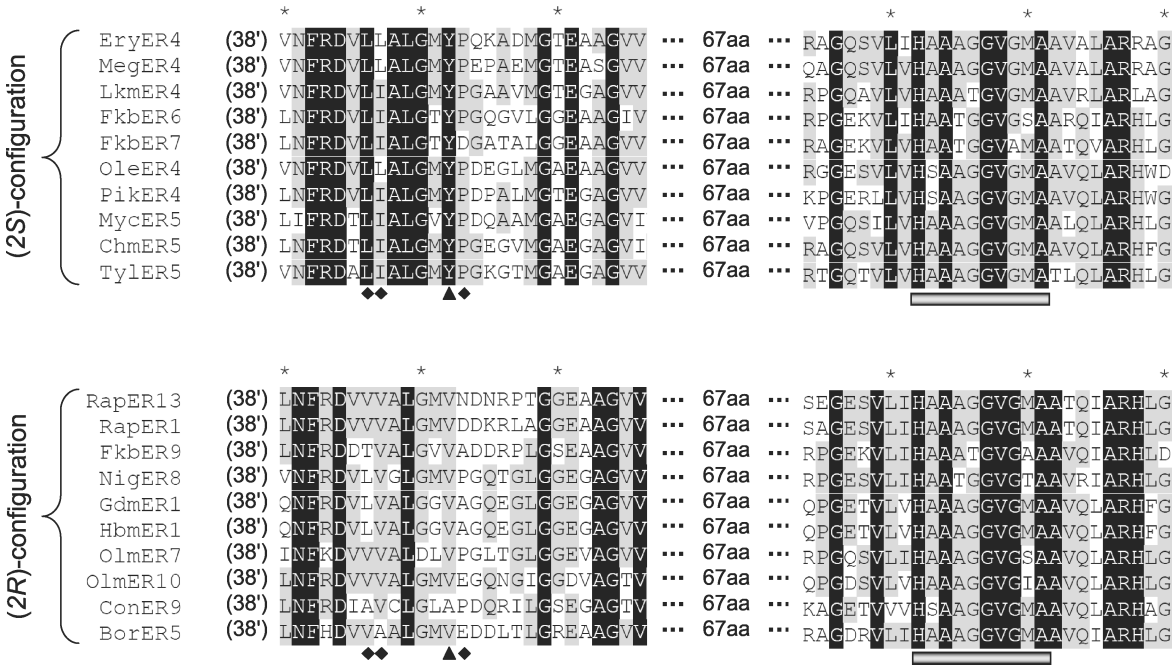

Figure 2. Sequence alignment of a portion of representative ER domains from modular PKSs. The position of the unique tyrosine (Tyr52′) residue correlated with (2*S*) configuration in the polyketide product is marked with black triangles. Additional residues that may influence stereospecificity are marked with black diamonds. The position of the NADPH binding site is marked with gray bars. Residue numbering is based on that of *E. coli* QOR (PDB ID 1QOR) on which the ER domains were modeled.

RESULTS AND DISCUSSION

Probing the Contributions of Active Site Residues to Stereospecificity in a PKS Enoylreductase (ER) Domain. The model system we previously used to test the role in ER stereospecificity of the residue at position 52′ was a bimodular recombinant PKS (Figure 1) derived from DEBS1-TE (*20*), a recombinant PKS consisting of the loading module and first two extension modules of the erythromycin PKS (DEBS). When the $EryKR_2$ domain housed in DEBS1-TE was replaced with either the full set of reductive domains of module 4 of DEBS or the full set of reductive domains of module 13 of the rapamycin PKS (RAPS), the resulting recombinant PKSs, referred to here as TKS-ery4 and TKS-rap13, produced the reduced triketides **1** and **2**, respectively (*19, 21*). While mutagenesis of Tyr to Val in position 52′ of $EryER_4$ was successful in the TKS-ery4 system in switching the stereochemistry of enoylreduction, resulting in a major product **2** (whereas for the parent, unmutated enzyme, the major product is **1**), mutation of Val to Tyr in position 52′ of $RapER_{13}$ of TKS-rap13 did not change the stereochemistry of enoylreduction and both parent and mutant enzymes catalyzed the formation of **2** as the major product. Clearly residues other than residue 52′ help determine the stereospecificity of the ER domain.

Further analysis of multiple sequence alignments of authentic ER domains suggested additional potentially important residues: for example, at residue 53′ proline is present in over 90% of the ER domains known to catalyze enoylreduction yielding the (2*S*) configuration. Among the ER domains known to produce the (2*R*) configuration, proline is present at position 53′ only 50% of the time (Figure 2). We therefore constructed a double mutant bearing the mutations V52′Y and N53′P in the $RapER_{13}$ domain of TKS-rap13. The mutant gene was introduced into *Saccharopolyspora erythraea* BIOT1717-JC2. However, after fermentation, LC−MS analysis of extracts from the transformant revealed that there is no switch in the methyl configuration of the triketide lactone, and **2** remains the major product (Figure 3, panel A), showing that additional alteration in residue 53′ had made no difference to the stereochemical outcome. Meanwhile, residues 46′ and 47′ in the ER domains that produce the (2*S*) configuration are typically con-

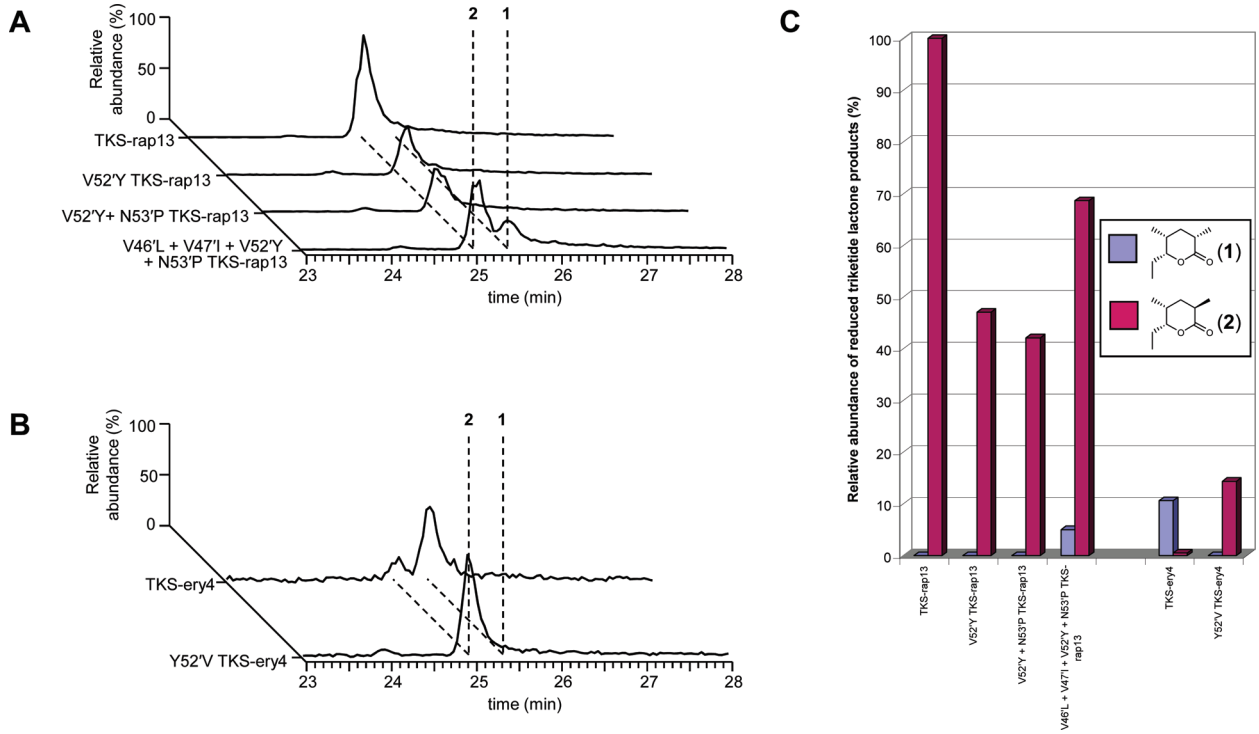

Figure 3. Reduced triketide lactone diastereoisomers produced from engineered triketide synthases. A) LC–MS chromatograms of the products of *S. erythraea* BIOT1717-JC2 containing TKS-rap13 and mutants. The parent enzyme and V52′Y and V52′Y + N53′P mutants produce 2 as the sole reduced triketide, but the L46′V + I47′V + V52′Y + N53′P mutant produced 1 as a minor and 2 as a major product. B) LC–MS chromatograms of the products of *S. erythraea* BIOT1717-JC2 containing TKS-ery4 and the Y52′V mutant. The parent enzyme produces 1 (major) and 2 (minor), but the Y52′V mutant produces 2 as the only reduced triketide product (*19*). C) The relative abundance of reduced triketide diastereomers from *S. erythraea* BIOT1717-JC2 containing TKS-rap13, TKS-ery4, and mutants derived from them (*19*).

served as Leu and Ile, respectively, with Leu46′ being more strongly conserved. In the ER domains that produce the (2*R*) configuration, however, these positions are more frequently occupied by less bulky Val residues (Figure 2). Our model suggests that these positions are situated in the vicinity of the active site. Residues flanking these positions did not correlate with stereochemical outcome. The mutations V46′L, V47′I, V52′Y, and N53′P were accordingly introduced together into the $RapER_{13}$ domain of TKS-rap13, and the mutant gene was introduced into *S. erythraea* BIOT1717-JC2. Analysis of the fermentation products by LC–MS revealed a small but detectable shift in stereospecificity: a new peak was observed in the chromatogram at the position of elution corresponding to **1**, but the major product was still **2** (Figure 3, panel A). This shift in stereochemical outcome, albeit less striking than that produced by substitution of residue 52′ in the engineered triketide synthase TKS-ery4, which contains the reductive domains of DEBS module 4 (Figure 3, panel B), is intriguing because it suggests that further incremental changes in the stereochemical outcome might be obtained by more systematic mutagenesis in this region of the active site, for example, by iterative saturation mutagenesis (*22*). A comparison of the relative abundance of reduced triketides from the engineered PKSs and mutants is shown in Figure 3, panel C.

Searching for Putative Catalytic Residues in the ER Domain of a Modular PKS. A satisfying model of catalysis by the KR domains of modular PKSs has previously been obtained by specific mutagenesis of conserved tyrosine, serine, and lysine residues modeled to be at the active site, leading to the unambiguous loss of KR activity (*9*). We sought likewise to identify potential ER catalytic residues within the active site of $RapER_{13}$ and to test the outcome of mutagenesis at these positions.

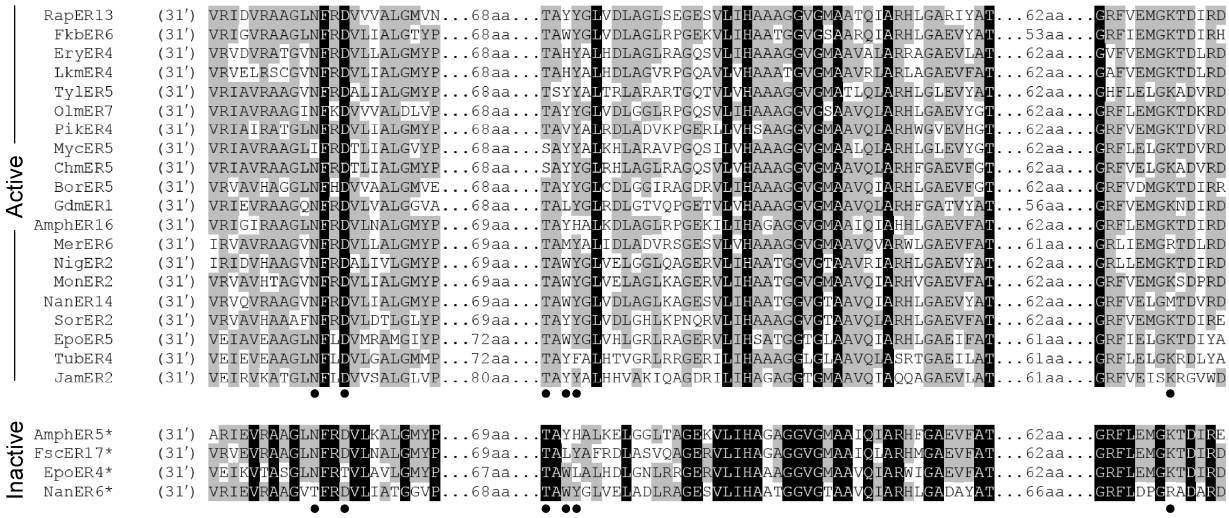

Figure 4. Sequence alignment of a portion of representative active ER domains and inactive ER domains. The positions of putative catalytic residues targeted for mutagenesis experiments are indicated with black circles.

We first searched for residues conserved in all active PKS ER domains, which were modeled to be in the vicinity of the active site, but which are not conserved in ER domains known to be inactive (Figure 4). Thus, the residue in position 41′ is conserved as an asparagine (with the apparent exception of the ER of module 5 of the mycinamicin PKS in which it is an isoleucine (*23*)), whereas in the inactive ER domain from module 6 of the nanchangmycin PKS ($NanER_6$), this position is instead occupied by a threonine (*24*). Similarly, in all known active ER domains, residue 43′ is invariably conserved as an aspartate, whereas in the inactive ER domain from module 4 of the epothilone PKS ($EpoER_4$), this position is taken by threonine (*25*). In the MDR family of enzymes to which the ERs of modular PKSs belong, it has been proposed that a conserved tyrosine, equivalent to position 125′ of the PKS ER domains in this discussion (corresponding to residue 130 in *E. coli* QOR), serves as a catalytic residue (*15*). Tyr125′ is also highly conserved in PKS ER domains and is lacking in two inactive ER domains from module 5 of the amphotericin PKS ($AmphER_5$) (*26*) and module 4 of the epothilone PKS ($EpoER_4$) (*25*). Against this, the apparently active ER domains from module 16 of the amphotericin PKS ($AmphER_{16}$) (*26*) and from module 4 of the tubulysin PKS ($TubER_4$) (*27*) also lack Tyr125′, although in those cases, the adjacent position 124′ is occupied by tyrosine. Overall, these multiple alignments therefore could not provide clear-cut candidates for ER active-site residues that might play direct catalytic roles.

From our homology model (*19*) of the PKS ER, the conserved threonine or serine residue at position 122′ lies within the active site, adjacent to the C-4′ of NADPH in an orientation that might allow catalytic function, and though it is found also in the inactive ER domains, its position and conservation made it an attractive candidate as a catalytic residue. Recent crystallographic studies of mammalian FAS have suggested that, in the ER domains of these highly homologous enzymes, conserved Lys1771 and Asp1797 residues are potential donor residues to supply a proton at C-2 during enoylreduction (*17*). However, the region containing Asp1797 in mammalian FAS does not align either with $RapER_{13}$ or with the ER sequences from other modular PKSs. Lys1771 of mammalian FAS does correspond to position 236′, which is typically conserved as a lysine or arginine in modular PKS ERs. Again, though, there are prominent exceptions: in the active ER domains of module 14 of the nanchangmycin PKS ($NanER_{14}$) (*24*) and of module 7 of the tubulysin PKS ($TubER_7$) (*27*), this position is occupied by methionine and valine, respectively.

In summary, six candidate catalytic residues were identified in the above analysis (Asn41′, Asp43′, Thr122′, Tyr124′, Tyr125′, and K236′) (Figure 5) of which only Asp43′ is fully conserved in all apparently active PKS ER domains (though when Thr122′ is absent, it is replaced by a similar residue, Ser). Intrigued by this

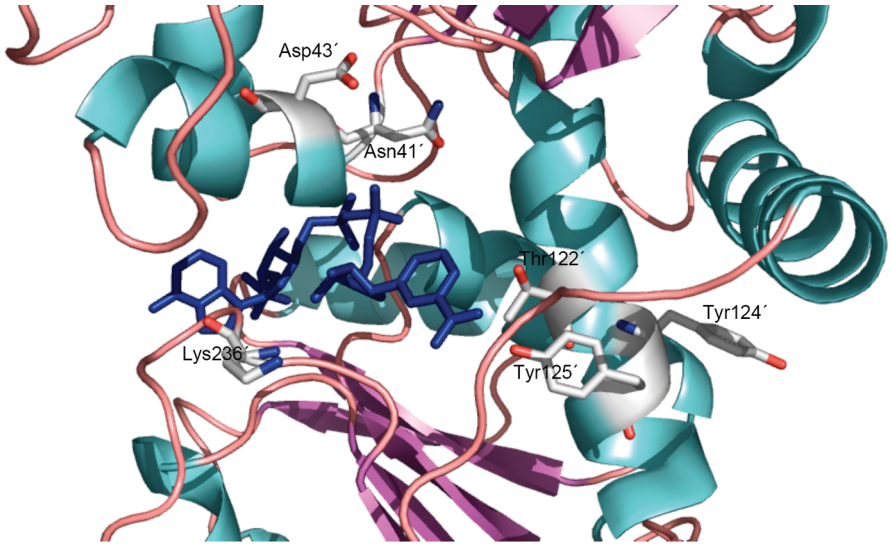

Figure 5. Model of $RapER_{13}$ showing active site residues targeted for mutagenesis. The side chains of the targeted residues are shown, The NADPH cofactor is shown in blue.

observation, we undertook specific mutagenesis of these residues in the $RapER_{13}$ domain and measured the effect on catalysis.

Mutagenesis of Putative Catalytic Residues. Mutants were constructed in the model triketide lactone synthase, TKS-Rap13, as described previously (*19, 21*). Asn41′, Asp43′, Thr122′, Tyr124′, Tyr125′, and Lys236′ were mutated either individually or in combination (Table 1). Plasmids housing these mutants were introduced into the host strain *S. erythraea* BIOT1717-JC2, and titers of triketide lactone were then determined by LC–MS analysis of the culture extracts after fermentation for 10 days (Figure 6). Most of the strains housing the TKS-rap13 mutants produced, in diminished amounts compared to the parent strain, the fully reduced triketide lactone **2** or, in the case of the K236′A mutant described below, both diastereomers **1** and **2**. However, in none of the strains was the production of the fully reduced triketide lactone completely abolished. Each of the mutants also produced a proportion of unreduced 3-keto triketide lactone (**3**) in similar amounts, and thus the relative ratio of fully reduced to unreduced triketide lactone was also compared between the mutants, which showed that although the

TABLE 1. Mutations of candidate catalytic residues

Mutation	Rationale
N41′A	Conserved Asn absent in inactive $NanER_6$ (*23*) — alanine mutation
N41′D	Conserved Asn absent in inactive $NanER_6$ (*23*) — isosteric mutation
N41′T	Conserved Asn absent in inactive $NanER_6$ (*23*) — changed to match $NanER_6$
D43′A	Conserved Asp absent in inactive $EpoER_4$ (*24*) — alanine mutation
D43′N	Conserved Asp absent in inactive $EpoER_4$ (*24*) — isosteric mutation
D43′T	Conserved Asp absent in inactive $EpoER_4$ (*24*) — changed to match $EpoER_4$
T122′V	Positioned in active site of homology model
Y124′F	Aligns with proposed catalytic residue Tyr130 in *E. coli* QOR (*15*)
Y125′F	Aligns with proposed catalytic residue Tyr130 in *E. coli* QOR (*15*)
T122′V+Y125′F	Possible co-operativity between Thr122′ and Tyr125′
Y124′F	Possible co-operativity between Thr124′ and Tyr125′
K236′A	Aligns with proposed catalytic residue Lys1771 in mammalian FAS ER (*17*)

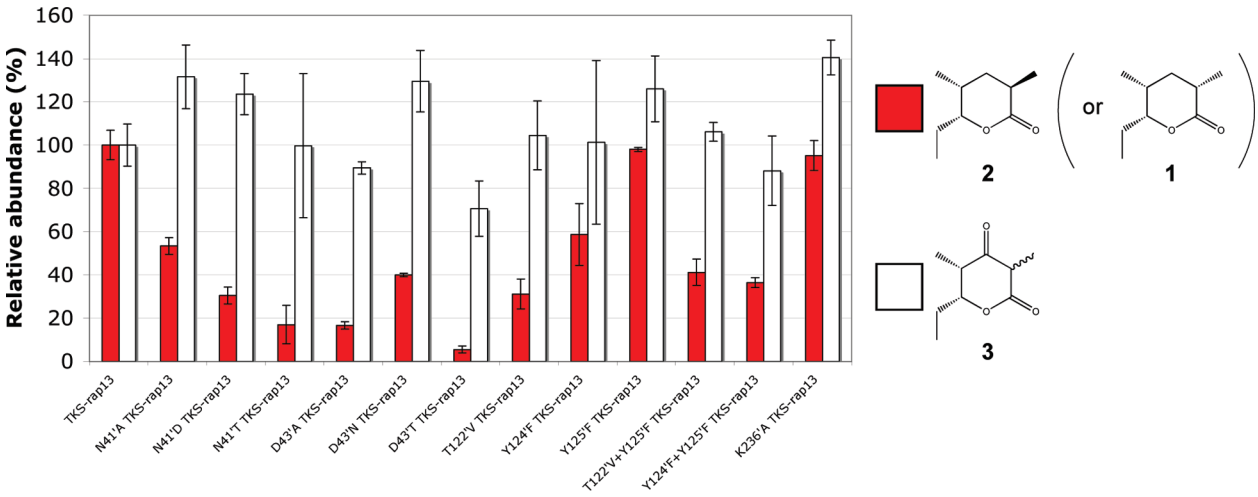

Figure 6. Levels of reduced and unreduced triketide lactones produced by TKS-rap13 variants expressed in *S. erythraea* BIOT1717-JC2. Reduced triketide 2 (or 1), saturated at the C-3 position, is shown in red, and 3-keto unreduced triketide 3 is shown in white.

amount of unreduced 3-keto triketide lactone **3** typically was comparable between mutant strains, significant differences in the production of fully reduced triketide lactone **2** were observed (Figure 6).

Asn41′ was replaced with either alanine, aspartate, or threonine (the residue found in the inactive $NanER_6$). The N41′A mutant produced **2** at a level of (53 ± 4)% of the levels from the parent strain, whereas the N41′D and N41′T mutants produced (30 ± 4)% and (17 ± 9)% compared to the parent strain, respectively. Likewise, several mutants were generated in which Asp43′ was replaced with alanine, asparagine or threonine (the residue found in the inactive $EpoER_4$). The D43′A mutant produced **2** at a level of (17 ± 2)% of the parent strain, whereas the D43′N and D43′T mutants produced (40 ± 1)% and (6 ± 2)% of the level in the parent strain respectively. The mutations at positions 41′ and 43′ that most diminished production of the reduced triketide lactone were replacements with threonine, the residue found at those positions in the inactive ERs $NanER_6$ (*24*) and $EpoER_4$ (*25*).

Thr122′, Tyr124′, and Tyr125′, which homology modeling placed at the ER active site (Figure 5), were also mutated. The T122′V and Y124′F mutants had diminished production of **2**, (31 ± 7)% and (59 ± 14)%, respectively, compared to that of the parent strain, and no significant decrease was observed in the Y125′F mutant, which produced (98 ± 1)% of the levels produced by the parent. The double mutants T122′V+Y125′F and Y124′F+Y125′F produced decreased amounts of (41 ± 6)% and (36 ± 2)% of **2** compared to the parent strain. These results were surprising because Tyr125′ is highly conserved among MDRs and given that its position in models of $EryER_4$ and $RapER_{13}$ and the position of the corresponding residue in the crystal structure of the related *E. coli* QOR suggest that it is favorably placed to play a direct role in catalysis (*15*). Because none of these mutations abolish production of **2** or result in levels of production lower than ~30% of the parent strain, it is clear that in the PKS ER Tyr125′ is not an essential catalytic residue.

Surprisingly, mutagenesis of Lys236′ in TKS-rap13, which corresponds to the Lys1771 proposed as a catalytic residue in the mammalian FAS (*17*), had no effect on the production of the reduced triketide lactone, the K236′A mutant producing (95 ± 7)% of wild type levels. Clearly, this residue is not essential for enoylreduction in modular PKSs. Interestingly, however, the mutation did result in a shift in the stereospecificity of the enzyme, with **1** being produced as well as **2**, in a proportion of 1:6 (Figure 7). Although Lys236′ is demonstrably nonessential in this ER, it nevertheless might act here as a proton donor to C-2: in the mutant where this base is missing, there would likely be less control over the direction of protonation, and a solvent-derived proton might be delivered to either face of the carbanion intermediate.

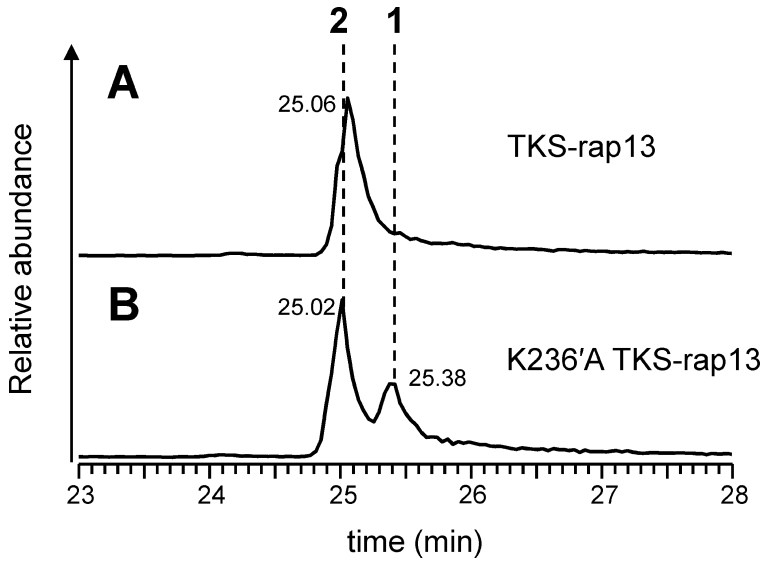

Figure 7. LC−MS chromatograms of triketide lactones produced by *S. erythraea* BIOT1717-JC2 containing TKS-rap13 variants. Fermentation extracts were from *S. erythraea* strains housing (A) TKS-rap13 and (B) K236′A TKS-rap13.

Concluding Remarks. Previously we demonstrated that, in a bimodular PKS (TKS-ery4) that contains the KR, DH, and ER of DEBS module 4, a single mutation (Y52′V) changes the $EryER_4$ from being stereospecific for the formation of a (2*S*)-methyl branched product to being stereospecific for the formation of a (2*R*) product (*19*). In contrast, in TKS-rap13, which contains the reductive domains of RAPS module 13 in which $RapER_{13}$ is normally specific for reduction to the (2*R*) product, the corresponding mutation (V52′Y) resulted in no observable change in stereospecificity. Here, we have shown that when further residues thought to lie near the active site of TKS-rap13 were simultaneously mutated (V46′L + V47′I + V52′Y + N52′P) to match the consensus of the (2*S*) specific ER domains, a small shift in stereospecificity of the $RapER_{13}$ could now be detected. The correlation between ER sequence and stereochemical outcome may prove to be useful information for future genetic sequence-based prediction of natural product configuration. Recently, the ability to predict KR stereospecificity has been used to aid in assigning the configuration of the polyketide natural products chivosazol A (*28*), etnangien (*29*), and salinilactam A (*30*), where predictions of hydroxyl stereochemistry based upon genetic sequence were confirmed by NMR and classical synthetic and degradation studies.

Our extensive mutagenic analysis of the $RapER_{13}$ active site has, surprisingly, failed to reveal a single residue that is essential for activity when assayed by the production of a polyketide *in vivo*. This result was foreshadowed by our observation that only one of these candidate residues is fully conserved in all active PKS ER domains (Asp43′). We considered the possibility of an adventitious ER activity operating in *trans* in *S. erythraea* to take over the function of an essential ER active site residue. However, this explanation is unlikely because in the same model triketide synthase system in *S. erythraea* we have previously found that an engineered second extension module containing KR and DH gave rise exclusively to the predicted 2-enoate product, ruling out the presence in these cells of such a *trans*-acting ER activity (*21*). Consistent with this, mutagenesis of the NADPH-binding site in the DEBS ER in *S. erythraea* also led to complete ablation of this ER activity, with no observable contribution from a *trans*-acting ER (*31*). In particular, our findings undermine the idea that Tyr125′ (corresponding to Tyr130 in *E. coli* quinone oxidoreductase 1QOR), which is conserved in the MDR family of enzymes, plays an essential catalytic role in ER catalysis (*15*). If Lys236′ does act as a proton donor to C-2, as proposed for the equivalently positioned lysine residue in the mammalian FAS (*17*), then another as yet unidentified base must be able to take over this function in the K236′A mutant.

METHODS

Additional details for the experimental procedures are available in the Supporting Information.

Construction of Plasmids. The DNA encoding the complete set of reductive domains of module 13 of the rapamycin PKS, including the engineered flanking restriction sites *Avr*II and *Hpa*I (*21*), was PCR amplified from the plasmid pDK19.0, encoding TKS-rap13, with the primers GACCGTCGACGACGCCGAGTC and GGTCAGCGAGTCGAAGCCGAGC and subcloned into pUC18

via the blunt-cutting *Sma*I site. This plasmid was then used as a template for site directed mutagenesis at a number of different amino acid positions using mutagenic primers (see Supporting Information). The DNA encoding the set of reductive domains with the mutagenized ER domain was excised by restriction digestion from each of the resulting pUC18-derived plasmids as an *Avr*II-*Hpa*I fragment and ligated to pDK19.0 cut with the same enzymes. The resulting plasmids encoded various mutants of TKS-rap13 (see Supporting Information).

Manipulation and Handling of Bacterial Strains. *E. coli* was routinely grown in 2TY broth (1.6% tryptone, 1% yeast extract, 0.5% NaCl, supplemented with the appropriate selective antibiotics) at 37 °C and maintained or transformed by standard procedures (*32*). *E. coli* ET12567/pUZ8002 (*33*) was used for conjugation, and *E. coli* DH10B was used for general cloning purposes.

Plasmids were introduced into *S. erythraea* BIOT1717-JC2 by conjugation (*33*). For strain maintenance and growth of cultures for the isolation of genomic DNA, TSB (tryptic soy broth supplemented with the appropriate selective antibiotics) was used. The transformants were verified by isolation of genomic DNA (*34*) and PCR amplification of the DNA encoding $RapER_{13}$ followed by DNA sequencing of the PCR amplicon. For the growth of production cultures for analysis of triketide lactone production, EryP medium (*35*) was used, which is a medium favoring erythromycin production in *S. erythraea*.

Analysis of Triketide Lactones. Triketide lactone production cultures were grown in 25 mL of EryP medium (inoculated from 1 mL of a 10 mL starter culture grown in TSB for 3 days). After 10 days of growth at 30 °C, triketide lactones were extracted from the production cultures with 25 mL of ethyl acetate containing 1.6% formic acid. The organic solvent was removed from extracts *in vacuo*, and the residual oil dissolved in 1 mL of methanol for analysis by LC–MS, which was carried out on an Agilent 1200 HPLC system fitted with a Phenomenex ODS column (250 mm × 2.00 mm, 5 μm) and a Finnigan LTQ mass spectrometer system. The mobile phase used was a linear gradient from 95% water, 5% acetonitrile, 0.1% formic acid to 30% water, 70% acetonitrile, 0.1% formic acid over 35 min.

Acknowledgment: The authors thank Bojana Popovic for producing a homology model of the $RapER_{13}$ domain, and Frank Schulz for his helpful comments on the manuscript. This work was supported by a project grant from the Biotechnology and Biological Sciences Research Council (UK) to PFL (BB/D018943/1). D.H.K. was supported by a grant from the Cambridge Commonwealth Trust and a Post-Graduate Scholarship from Natural Science and Engineering Research Council of Canada and an Overseas Research Scholarship from Universities UK. P.F.L. and D.H.K. designed the study, and D.H.K carried out the experimental work and wrote the manuscript. D.H.K. thanks Cecilia A. Chen for her measureless support and encouragement.

Supporting Information Available: This material is available free of charge *via* the Internet at http://pubs.acs.org.

REFERENCES

1. Staunton, J., and Weissman, K. J. (2001) Polyketide biosynthesis: a millennium review, *Nat. Prod. Rep. 18*, 380–416.
2. Cortés, J., Haydock, S. F., Roberts, G. A., Bevitt, D. J., and Leadlay, P. F. (1990) An unusually large multifunctional polypeptide in the erythromycin-producing polyketide synthase of *Saccharopolyspora erythraea*, *Nature 348*, 176–178.
3. Smith, S., and Tsai, S.-C. (2007) The type I fatty acid and polyketide synthases: a tale of two megasynthases, *Nat. Prod. Rep. 24*, 1041–1072.
4. Lowden, P. A. S., Wilkinson, B., Böhm, G. A., Handa, S, Floss, H. G., Leadlay, P. F., and Staunton, J. (2001) Origin and true nature of the starter unit for the rapamycin polyketide synthase, *Angew. Chem., Int. Ed. 40*, 777–779.
5. Olano, C., Wilkinson, B., Sánchez, C., Moss, S. J., Sheridan, R., Math, V., Weston, A. J., Braña, A. F., Martin, C. J., Oliynyk, M., Méndez, C., Leadlay, P. F., and Salas, J. A. (2004) Biosynthesis of the angiogenesis inhibitor borrelidin by *Streptomyces parvulus* Tü4055: cluster analysis and assignment of functions, *Chem. Biol. 11*, 87–97.
6. Chan, Y. A., Podevels, A. M., Kevany, B. M., and Thomas, M. G. (2009) Biosynthesis of polyketide synthase extender units, *Nat. Prod. Rep 26*, 90–114.
7. Weissman, K. J., and Leadlay, P. F. (2005) Combinatorial biosynthesis of reduced polyketides, *Nat. Rev. Microbiol. 3*, 925–936.
8. Caffrey, P. (2003) Conserved amino acid residues correlating with ketoreductase stereospecificity in modular polyketide synthases, *ChemBioChem 4*, 649–662.
9. Reid, R., Piagentini, M., Rodriguez, E., Ashley, G., Viswanathan, N., Carney, J., Santi, D. V., Hutchinson, C. R., and McDaniel, R. (2003) A model of structure and catalysis for ketoreductase domains in modular polyketide synthases, *Biochemistry 42*, 72–79.
10. Siskos, A., Baerga-Ortiz, A., Bali, S., Stein, V., Mamdani, H., Spiteller, D., Popovic, B., Spencer, J. B., Staunton, J., Weissman, K. J., and Leadlay, P. F. (2005) Molecular basis of Celmer's rules: stereochemistry of catalysis by isolated ketoreductase domains from modular polyketide synthases, *Chem. Biol. 12*, 1145–1153.
11. Baerga-Ortiz, A., Popovic, B., Siskos, A. P., O'Hare, H. M., Spiteller, D., Williams, M. G., Campillo, N., Spencer, J. B., and Leadlay, P. F. (2006) Directed mutagenesis alters the stereochemistry of catalysis by isolated ketoreductase domains from the erythromycin polyketide synthase, *Chem. Biol. 13*, 277–285.
12. O'Hare, H. M., Baerga-Ortiz, A., Popovic, B., Spencer, J. B., and Leadlay, P. F. (2006) High throughput mutagenesis of active site residues to evaluate models of stereochemical control in ketoreductase domains from the erythromycin-producing polyketide synthase, *Chem. Biol. 13*, 287–296.
13. Keatinge-Clay, A. T., and Stroud, R. M. (2006) The structure of a ketoreductase determines the organization of the beta-carbon processing enzymes of modular polyketide synthases, *Structure 14*, 737–748.
14. Keatinge-Clay, A. T. (2007) A tylosin ketoreductase reveals how chirality is determined in polyketides, *Chem. Biol. 14*, 898–908.
15. Persson, B., Zigler, J. S., and Jörnvall, H. (1994) A super-family of medium-chain dehydrogenase/reductases (MDR), *Eur. J. Biochem. 226*, 15–22.
16. Nordling, E., Jörnvall, H., and Persson, B. (2001) Medium chain dehydrogenase/reductase (MDR). Family characterizations including genome comparisons and active site modeling, *Eur. J. Biochem. 269*, 4267–4276.
17. Maier, T., Leibundgut, M., and Ban, N. (2008) The crystal structure of a mammalian fatty acid synthase, *Science 321*, 1315–1322.
18. Anderson, V. E., and Hammes, G. G. (1984) Stereochemistry of the reactions carried out by chicken liver fatty acid synthase, *Biochemistry 23*, 2088–2094.
19. Kwan, D. H., Sun, Y., Schulz, F., Hong, H., Popovic, B., Sim-Stark, J. C. C., Haydock, S. F., and Leadlay, P. F. (2008) Prediction and manipulation of the stereospecificity of enoylreductase domains in modular polyketide synthases, *Chem. Biol. 15*, 1231–1240.
20. Cortés, J., Wiesmann, K. E. H., Roberts, G. A., Brown, M. J. B., Staunton, J., and Leadlay, P. F. (1995) Repositioning of a domain in a modular polyketide synthase to promote specific chain cleavage, *Science 268*, 1487–1489.
21. Kellenberger, L., Galloway, I. S., Sauter, G., Böhm, G., Hanefeld, U., Cortés, J., Staunton, J., and Leadlay, P. F. (2008) A polylinker approach to reductive loop swaps in modular polyketide synthases, *ChemBioChem 9*, 2740–2749.

22. Reetz, M., and Carballeira, J. D. (2007) Iterative saturation mutagenesis (ISM) for rapid directed evolution of functional enzymes, *Nat. Protoc. 2*, 891–903.
23. Anzai, Y., Saito, N., Tanaka, M., Kinoshita, K., Koyama, Y., and Kato, F. (2003) Organization of the biosynthetic gene cluster for the polyketide macrolide mycinamicin in *Micromonospora griseorubida*, *FEMS Microbiol. Lett. 218*, 135–141.
24. Sun, Y., Zhou, X., Dong, H., Tu, G., Wang, M., Wang, B., and Deng, Z. (2003) A complete gene cluster from *Streptomyces nanchangensis* NS3226 encoding biosynthesis of the polyether ionophore nanchangmycin, *Chem. Biol. 10*, 431–441.
25. Tang, L., Shah, S., Chung, L., Carney, J., Katz, L., Khosla, C., and Julien, B. (2000) Cloning and heterologous expression of the epothilone gene cluster, *Science 287*, 640–642.
26. Caffrey, P., Lynch, S., Flood, E., Finnan, S., and Oliynyk, M. (2001) Amphotericin biosynthesis in *Streptomyces nodosus*: deductions from analysis of polyketide synthase and late genes, *Chem. Biol. 8*, 713–723.
27. Sandmann, A., Sasse, F., and Müller, R. (2004) Biosynthetic machinery of tubulysin, a potent cytotoxin with potential anticancer activity, *Chem. Biol. 11*, 1071–1079.
28. Janssen, D., Albert, D., Jansen, R., and Müller, and Kalesse, M. (2007) Chivasazole A—elucidation of the absolute and relative configuration, *Angew. Chem., Int. Ed. 46*, 4898–4901.
29. Menche, D., Arikan, F., Perlova, O., Horstmann, N., Ahlbrecht, W., Wenzel, S. C., Jansen, R., Irschik, H., and Müller, R. (2008) Stereochemical determination and complex biosynthetic assembly of entangien, a highly potent RNA polymerase inhibitor from the myxobacterium *Sorangium cellulosum*, *J. Am. Chem. Soc. 130*, 14234–14243.
30. Udwary, D. W., Zeigler, L., Asolkar, R. N., Singan, V., Lapidus, A., Fenical, W., Jensen, P. R., and Moore, B. S. (2007) Genome sequencing reveals complex secondary metabolome in the marine actinomycete *Salinispora tropica*, *Proc. Natl. Acad. Sci. U.S.A. 104*, 10376–10381.
31. Donadio, S., McAlpine, J. B., Sheldon, P. J., Jackson, M., and Katz, L. (1993) An erythromycin analog produced by reprogramming of polyketide synthesis, *Proc. Natl. Acad. Sci. U.S.A. 90*, 7119–7123.
32. Ausubel, F. M., Brent, R., Kingston, R. E., Moore, D. D., Seidman, J. G., Smith, J. A., Struhl, R., Eds. (2002) *Short Protocols in Molecular Biology*, John Wiley & Sons, Inc., Toronto.
33. Kieser, T., Bibb, M. J.. Buttner, M. J., Chater, K. F., Hopwood, D. A. (2000) *Practical Streptomyces Genetics*, The John Innes Foundation, Norwich.
34. Pospiech, A., and Neumann, B. (1995) A versatile quick-prep of genomic DNA from gram-positive bacteria, *Trends Genet. 11*, 217–218.
35. Rowe, C. J., Cortés, J., Gaisser, S., Staunton, J., and Leadlay, P. F. (1998) Construction of new vectors for high-level expression in actinomycetes, *Gene 216*, 215–223.